

# Estimating the Degree of Nonlinearity in Transient Responses with Zeroed Early-Time Fast Fourier Transforms

Matthew S. Allen  
*Assistant Professor*  
*Department of Engineering Physics*  
*University of Wisconsin-Madison*  
*535 Engineering Research Building*  
*1500 Engineering Drive*  
*Madison, WI 53706-1609*  
[msallen@engr.wisc.edu](mailto:msallen@engr.wisc.edu)

&

Randall L. Mayes  
*Distinguished Member of Technical Staff*  
*Sandia National Laboratories\**  
*PO Box 5800*  
*Albuquerque, NM 87185*  
[rlmayes@sandia.gov](mailto:rlmayes@sandia.gov)

## Abstract:

This work presents time-frequency signal processing methods for detecting and characterizing nonlinearity in transient response measurements. The methods are intended for systems whose response becomes increasingly linear as the response amplitude decays. The discrete Fourier Transform of the response data is found with various sections of the initial response set to zero. These frequency responses, dubbed Zeroed Early-time Fast Fourier Transforms (ZEFFTs), acquire the usual shape of linear Frequency Response Functions (FRFs) as more of the initial nonlinear response is nullified. Hence, nonlinearity is evidenced by a qualitative change in the shape of the ZEFFT as the length of the initial nullified section is varied. These spectra are shown to be sensitive to nonlinearity, revealing its

---

\* Sandia is a multiprogram laboratory operated by Sandia Corporation, a Lockheed Martin Company, for the United States Department of Energy's National Nuclear Security Administration under Contract DE-AC04-94AL85000.

presence even if it is active in only the first few cycles of a response, as may be the case with macro-slip in mechanical joints. They also give insight into the character of the nonlinearity, potentially revealing nonlinear energy transfer between modes or the modal amplitudes below which a system behaves linearly. In some cases one can identify a linear model from the late time, linear response, and use it to reconstruct the response that the system would have executed at previous times if it had been linear. This gives an indication of the severity of the nonlinearity and its effect on the measured response. The methods are demonstrated on both analytical and experimental data from systems with slip and impact nonlinearities.

## **1. Introduction**

The vast majority of structural dynamic systems are modeled as linear and time invariant, in part because this class of systems is well understood and a number of powerful tools are available for their analysis. There is often a need to perform experiments to determine whether a given system can be adequately modeled as linear. Since all real systems are nonlinear, this boils down to estimating the error that may be introduced by approximating a nonlinear system as linear. In the event that testing reveals that the system of interest cannot be adequately modeled as linear, one would often also like to identify the nature of the nonlinearity.

This work is motivated by recent experiences testing and modeling components that are subjected to high amplitude shock loading. A variety of critical space and automotive systems are subjected to these types of loads. These components present quite a challenge in both testing and modeling especially if they contain mechanical joints. Bolted joints in these components may slip due to the high forces that the components experience, so they can no longer be treated as linear at high loads. Macro slip in joints is difficult to model because the force in the joint can be hysteretic in nature, depending not only on the displacement of the joint but on the past history of displacement. Also, the shock force may have high frequency content so many modes may be important when modeling or testing the component's response to the shock. This work presents a simple tool that helps one to evaluate the degree of nonlinearity induced in a subcomponent's response by impulsive loading.

Numerous methods have been proposed for detecting nonlinearity and for identifying parametric models of nonlinear systems, especially in the past few decades. Kerschen *et al* provide a thorough and recent survey of identification methods for nonlinear systems [1]. Many schemes are limited to persistent inputs, such as periodic, broadband random, etc..., but those cannot be used in this application for a number of reasons:

1. The components are designed to withstand shock inputs, so we desire to test them in a shock environment.
2. High-amplitude persistent inputs are much more expensive to apply than high level transient inputs.
3. Models derived through steady state testing may not accurately reproduce the response of the system to shock excitation.
4. The components may be destroyed or degraded by prolonged testing with high level periodic inputs.

The literature also contains a quite a few methods that are applicable to transient response data, as is of interest here, but each of these has limitations that preclude its use in this application. Some are essentially limited to SDOF or low order systems, such as the restoring force surface method [2, 3], others, such as the NARMAX approach, do not provide much physical insight. Other promising methods for the application of interest involve time-frequency analysis [4] and the Hilbert Transform [5]. The Hilbert Transform can be used to detect the instantaneous frequency and decay envelope of a signal, which are related to the instantaneous stiffness and damping respectively, but it is limited to mono-component or single degree of freedom systems. One potential alternative [6] requires enough sensors to construct a modal filter [7, 8], which precludes its use in this work. Other approaches, such as the Hilbert-Huang Transform (HHT) [5, 9] show promise, but are not yet fully developed.

Various types of time-frequency analysis techniques have been proposed, such as the short time Fourier transform (STFT), Choi-Williams expansion, and wavelets. These are problematic in the application of interest because the window functions that they employ reduce the influence of very short transients, but the slipping nonlinearities in the systems of interest may only be active in the first few cycles of the response. There are also always limitations in the frequency resolution that can be obtained with any time-frequency method. However, the biggest difference between time-frequency methods and the methods presented here is that the spectra obtained by time-frequency methods have different

customary shapes than the frequency response functions that most dynamicists are accustomed to, so insight gleaned from experience with linear systems may be difficult to transfer to the time-frequency spectra of the nonlinear response. The methods presented in this work utilize the free response of a system and its Fourier Transform, which, for a linear system, have the same mathematical form as the impulse response and frequency response. As a result, the spectra are similar to linear frequency response functions, which are familiar to most dynamicists. The methods presented here are also capable of handling relatively high order systems; they can be applied to virtually any response.

The approach presented here involves finding the discrete Fourier Transform of the response data with various sections of the initial response set to zero. The resulting frequency-domain responses, which are named Zeroed Early-time Fast Fourier Transforms or (ZEFFTs) in this work, take on the usual shape of linear Frequency Response Functions (FRFs) as more of the initial nonlinear response is nullified. By comparing multiple ZEFFTs, each created with a different portion of the initial nonlinear response nullified, one observes changes in the shape of the spectrum as the nonlinear response decays to the low-amplitude linear response. A few tools are presented to aide in interpreting the results, and a metric is presented that describes how important the nonlinearity is to the response. Because this method assumes that the nonlinearity is active early in a response and disappears, one may have to use care to avoid mistaking heavily damped modes with nonlinearity for some systems. The examples presented here highlight the key issues for simulated systems whose linear modes have damping ratios that differ as much as a factor of three between any two modes in the frequency band of interest, yet the methods still prove to be quite effective.

The following section presents the theory behind the nonlinear detection method. The method is applied to analytical data from a system with slip, contact and cubic nonlinearity in Section 3, and the limitations of the method in the presence of measurement noise are discussed. Section 4 presents the results of applying the algorithm to a rather complicated experimental measurement from a real system with a bolted joint. Finally, Section 5 presents some conclusions.

## 2. Proposed Tools and Theoretical Development

### 2.1. Zeroed Early-Time Fast Fourier Transforms (ZEFFTs)

It is well known that many nonlinear systems are increasingly well approximated as linear as their response amplitude diminishes. These systems are the focus of this work. Although nonlinear systems do not have linear modes of vibration, we shall speak of such in the following, and in all cases this should be interpreted to mean the modes of the small-amplitude, linearized system. The free response of the linearized system can be represented as a sum of decaying sinusoids, or complex exponentials, which in state space form [10] can be written as follows,

$$y(t) = \begin{cases} \sum_{r=1}^N R_r \exp(\lambda_r t) + R_r^* \exp(\lambda_r^* t) & t \geq 0 \\ 0 & t < 0 \end{cases} \quad (1),$$

where  $R_r$  and  $\lambda_r$  are the complex residue and eigenvalue respectively,  $()^*$  denotes complex conjugate and  $N$  is the number of modes active in the response. The common case of under-damped modes has been assumed, so the modal parameters occur in complex conjugate pairs with  $\lambda_r = -\zeta_r \omega_r + i \omega_r \sqrt{1 - \zeta_r^2}$  where  $\zeta_r$  is the  $r$ th damping ratio and  $\omega_r$  is the  $r$ th natural frequency. Equation (1) can be expressed in terms of real variables in the following form (which may be more familiar to some readers)

$$y(t) = \sum_{r=1}^N \exp(-\zeta_r \omega_r t) \left[ C_{1r} \sin(\omega_r t \sqrt{1 - \zeta_r^2}) + C_{2r} \cos(\omega_r t \sqrt{1 - \zeta_r^2}) \right]. \quad (2),$$

The complex constants  $R_r$ , or their real counterparts  $C_{1r}$  and  $C_{2r}$  depend on the initial position and velocity of the system. The Fourier transform of eq. (1) is the following,

$$Y(\omega) = \sum_{r=1}^N \left( \frac{R_r}{i\omega - \lambda_r} + \frac{R_r^*}{i\omega - \lambda_r^*} \right) \quad (3)$$

which has the same form as the standard pole-residue expression for the Frequency Response Function (FRF) of a linear system [10, 11], except that the definition of the residues is different. The residues affect only the modal amplitudes of the response, so, the shape of the spectrum near each peak is essentially the same as in an FRF but the peaks may have different heights. The zeros in the spectrum of the free

response depend on the coefficients  $R_r$  and hence on the initial conditions, so they are different than the zeros of an FRF.

Suppose one were to artificially set the linearized response in eq. (1) to zero up to some time which we shall denote  $t_z$ .

$$y_z(t) = \begin{cases} 0, & t < t_z \\ y(t), & t \geq t_z \end{cases} \quad (4)$$

The Fourier transform of the zeroed response is the same as in eq. (3), only the residues change to reflect the initial conditions at  $t_z$ . Specifically, the Fourier transform of  $y_z(t)$  is

$$Y_z(\omega) = \sum_{r=1}^N \left( \frac{R_r e^{\lambda_r t_z}}{i\omega - \lambda_r} + \frac{(R_r e^{\lambda_r t_z})^*}{i\omega - \lambda_r^*} \right) e^{i\omega t_z} . \quad (5)$$

The term  $\exp(i\omega t_z)$  introduces a linearly increasing phase on the responses and is a result of the well known time shifting property of the Fourier Transform. This can be easily eliminated by multiplying the frequency response by  $\exp(-i\omega t_z)$ . After doing so, the response  $Y_z(\omega)$  has the exact same functional form as  $Y(\omega)$ . Only the residues are different, so if one were to compare plots of  $Y_z(\omega)$  and  $Y(\omega)$ , the only difference would be in the magnitude and phase of the peaks and the locations of the zeroes.

The situation is dramatically different if the response is nonlinear. A generally valid expression analogous to eq. (1) does not exist for a nonlinear system, but it is well known that the Fourier Transform of the free response of a nonlinear response can be very different from that of a linear system. For example, the nonlinear forces may shift the frequencies in the response and additional harmonics may be present. However, if the nonlinearity decreases with amplitude, then the response of a nonlinear system can eventually be well approximated as linear if one disregards enough of the initial response (or sets it to zero). Once the nonlinear part of the response has been nullified, the remaining response obeys eq. (1) and the character of the spectrum would cease to change as more of the initial response is eliminated. This is the key to the zeroed-fast Fourier transform nonlinearity detection algorithm.

These concepts are applied systematically to detect and characterize nonlinearity as follows. Given a response of interest,  $y(t)$ , which is suspected to be nonlinear, one first selects a set of times at

which to zero the response, denoted  $t_k$ . Then, a set of zeroed responses  $y_k(t)$  are created by assigning a value of zero to the response up to  $t_k$ .

$$y_k(t) = \begin{cases} 0, & t < t_k \\ y(t), & t \geq t_k \end{cases} \quad (6)$$

The Discrete Fourier Transform (DFT) of each of these responses

$$Y_k(\omega) = \text{DFT}\{y_k(t)\} \quad (7),$$

is then found and the DFTs are compared. In some cases leakage may contaminate the DFT, yet one can minimize it by choosing  $t_k$  to be instants when the response is near zero. The spectra,  $Y_k(\omega)$ , are here dubbed Zeroed Early-Time FFTs (ZEFFTs) or zeroed FFTs. Nonlinearity can be detected by visually observing the ZEFFTs to see if the response is distorted around any of the low-amplitude natural frequencies, or if any additional frequency content is present in the early ZEFFTs that cannot be attributed to the linear system.

### Example:

The proposed method was applied to an experimentally measured response from a 305 mm long beam, which was bolted at one end to a 117 mm long beam, as shown in the schematic in Figure 1. This hardware and experiments were described in detail in [12, 13]. The short beam was struck with an instrumented hammer as indicated in the figure, with an impulse whose peak force was 845 N, and the response was recorded on the 305 mm long beam. The ZEFFTs of the response were created for various zero times and are shown in Figure 1 for frequencies near the second (linearized) mode of vibration. The color of the lines indicates the zero time  $t_k$  for that particular ZEFFT, and a legend is shown giving the times, in milliseconds for some of the ZEFFTs. The resonance frequency of the mode in focus seems to increase from about 1380 Hz to about 1403 Hz as the response amplitude diminishes, causing the peak for early zero times to broaden. This represents a shift of only 1.5%, yet one can clearly observe that the early response does not have the usual linear shape. (This could be confirmed by attempting to curve-fit the response at early times, which would reveal that a linear modal model with one mode can not be made to agree with the measurement.)

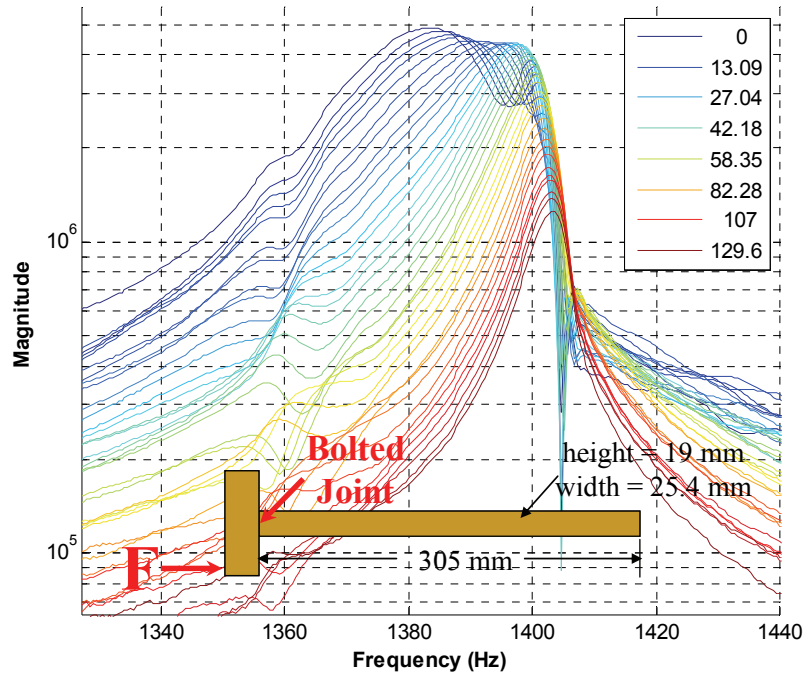


*Figure 1: ZEFFTs acquired from a T-beam with a bolted joint. The natural frequency of the mode in focus shifts causing a distortion in the response at early times. This distortion diminishes as the response decays, revealing that the beam is nonlinear and that this linearized mode softens with increasing amplitude.*

This nonlinearity detection approach relies on the fact that the nonlinearity in the response decays rather quickly with time. Some systems may contain certain linear modes that also decay very quickly with time, so it might be difficult to distinguish the two. Fortunately, shape of the frequency responses often allows one to determine whether a certain feature is actually just a heavily damped linear mode. For example, consider the 0 ms response in Figure 1. One might erroneously attribute this to two modes, a heavily damped mode with a natural frequency of 1380 Hz and a lightly damped mode whose frequency is 1403 Hz. However, if one were to construct a two-mode approximation to the 0ms response, one would see that the way that the shapes of the measured ZEFFTs evolve after 0 ms is not consistent with a two mode description. The tools presented in the following section aid one in assessing this and other issues.

## **2.2. Backwards Extrapolation for Nonlinearity Detection (BEND)**

In some instances it is not easy to visually discern nonlinear behavior from linear behavior. This section proposes an approach dubbed Backwards Extrapolation for Nonlinearity Detection (BEND), which



aids in visualizing the degree to which a nonlinear response deviates from linear behavior. The idea is to find a linear approximation to the system at later times (when it is thought to behave linearly) and then propagate that response backwards in time assuming linear behavior. Hence, one can compare the actual response of the system with an estimate of the response that the system would have had if it were linear.

The method for achieving this is actually quite simple. If the response after a certain instant,  $t_k$ , is approximately linear, then the corresponding zeroed response  $y_k$  can be fit to the form in Equation (1) (this response is zero for  $t \leq t_k$ ). This fitting process obtains the poles  $(\lambda_r)_k$  and residues  $(R_r)_k$  describing the response for  $t > t_k$  using one of the methods discussed in the following subsection. Now suppose that we want to propagate this response backwards to time  $t_1$  in order to compare it with the measured response truncated at  $t_1$ . Comparing Equations (3) and (5), the residues of the linear system at time  $t_1$ , denoted  $(R_r)_1$ , are related to those at time  $t_2$ , denoted  $(R_r)_2$  as follows:

$$(R_r)_2 = (R_r)_1 e^{\lambda_r(t_1-t_2)}. \quad (8)$$

The modal parameters  $(\lambda_r)_1$  and  $(R_r)_1$  can be used to reconstruct the linear approximation to the response in the time domain using eq. (1), or they can be used to reconstruct the ZEFFT  $Y_k^{lin}(\omega)$  using eq. (3) in the frequency domain.

### 2.3. Suitable Linear Response Identification Methods

A variety of methods exist that could be used to identify a linear pole-residue model from the responses at late times. Allemang and Brown [14] showed how most of these can be viewed in a common framework, and texts by Maia *et al* [15] and Ewins [16] review a number of methods. There are a few questions that one should consider for the present application.

- 1.) Does the algorithm return non-physical or computational modes?
- 2.) How accurately is damping estimated?
- 3.) Is the system identification algorithm robust to noise?

The first two are important in light of eq. (8), and considering the effect that the damping in each mode has on the extrapolation; error in the identified damping will directly affect the extrapolation. Some

algorithms introduce computational modes that are often either heavily damped or negatively damped [17], and this would clearly have an adverse affect on the extrapolation.

To circumvent these difficulties, the authors have used an iterative system identification algorithm that attempts to identify only the true physical modes of the system. The algorithm, dubbed the Algorithm of Mode Isolation (AMI), was first presented by Drexel and Ginsberg [18] and later extended and validated by Allen and Ginsberg [11, 19-23]. The algorithm works on frequency domain response data by identifying and subtracting modes from the data until it is reduced to noise (care is taken to avoid identifying and subtracting spurious modes), and the modes identified are then refined through an iterative procedure.

## 2.4. Single Trace Metric: Integral BEND (IBEND)

Sometimes it is desirable to have a simple metric quantifying nonlinearity. One such metric can be constructed by comparing the total area between the measured and reconstructed magnitude FRF curves over a specified frequency band. (The reconstructed FRF curves are found by identifying the linear system from the frequency response at a certain zero time and then propagating it forward and backward to all other times.) Let  $Y_k(\omega)$  and  $Y_k^{lin}(\omega)$  denote the measured and linearly extrapolated ZEFFTs associated with zero time  $t_k$ . The nonlinearity metric,  $IB(t_k)$ , dubbed the Integral of the Backwards Extrapolation for Nonlinear Detection (IBEND), is given by the following,

$$IB(t_k) = \frac{\int_{\omega_L}^{\omega_H} \left| |Y_k(\omega)| - |Y_k^{lin}(\omega)| \right| d\omega}{\int_{\omega_L}^{\omega_H} |Y_k(\omega)| d\omega} \quad (9)$$

where  $\omega_L$  and  $\omega_H$  denote the lower and upper frequency limits over which the integral is computed. For discrete measured data the integrals are computed for each zero time using trapezoidal integration. If the response at the time at which the curve fit was performed is truly linear, the metric  $IB(t_k)$  should be near zero for all times. As the IBEND curve is traced backwards in time, the first time encountered (latest time) at which its magnitude is significantly greater than zero indicates the end of nonlinear behavior. The accuracy of the system identification results can also be verified by observing that the metric remains

small at times in which the system is thought to behave linearly. This will be illustrated in the following sections.

### 3. Analytical Examples

The nonlinearity detection algorithm was tested by applying it to synthetic data from the seven degree-of-freedom system shown in Figure 2. The system consists of a small subsystem connected to a large master system through a nonlinear element. Because the attached system is small, the nonlinearity is most evident in the responses of the attached system. All of the masses are constrained to move in the x-direction only. The following parameters were used for the system:  $m_1$  through  $m_5 = 1$  kg,  $m_6 = m_7 = 0.1$  kg,  $k_1$  through  $k_4 = 1e6$  N/m,  $k_6 = 1e6$  N/m. Mass and Stiffness proportional damping was used (the nonlinear connection was not included in its calculation) with the following damping matrix:  $[C] = \alpha[M] + \beta[K]$  with  $\alpha = 8$ ,  $\beta = 0.00003$ , which gave modal damping ratios for the system (linearized about its static equilibrium) between 1.5% to 7.8%. Two different functions were used for the nonlinear restoring force  $k_5(x_6-x_2)$ , as discussed in the following subsections.

In both cases, the system was excited by applying a half-sine excitation pulse with 0.1 ms duration and with total energy  $E_{in}$  to mass 5. The values used for  $E_{in}$  were different for each type of nonlinearity, as discussed in the following subsections. To simulate a realistic scenario in the application of interest, it was assumed that only the acceleration of mass six ( $d^2x_6/dt^2$ ) was measured.

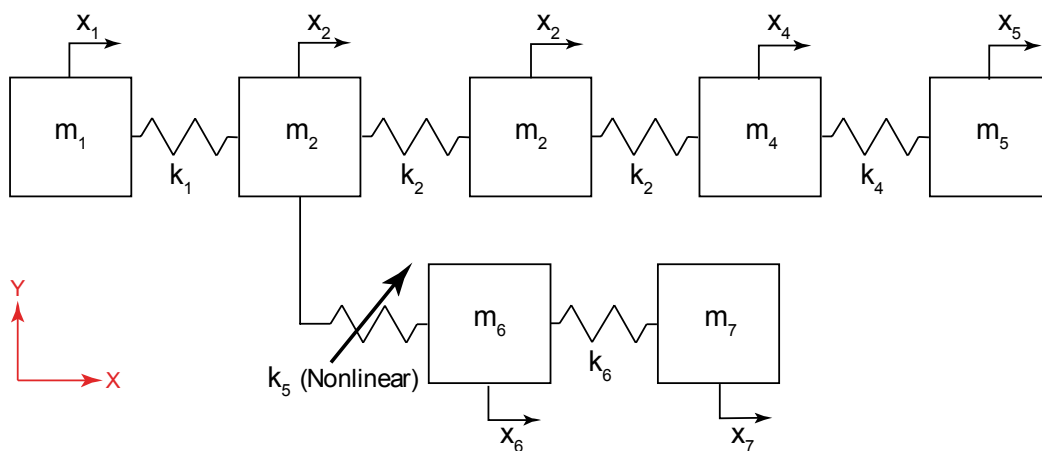


Figure 2: Seven DOF Mass-Spring System with a Nonlinear Connection

The following subsections describe the nonlinear force-displacement laws used for  $k_5$ , specifically: 1.) macro-slip nonlinearity (Jenkins element) and 2.) elastic impact type nonlinearity, and present the results of the proposed algorithms.

### 3.1. Slip Nonlinearity

For this case the connection between masses 2 and 6 was modeled using a Jenkins element [24] with a stiffness of  $1e6$  N and a slip force of  $1000$  N. The excitation energy was  $E_{in} = 3e9$  Joules, and the response of the system was found with a time step of  $1.221e-5$  using Euler's time integration method with a massless degree of freedom for the joint displacement. This system will be referred to as the slip system or the system with the slip nonlinearity from this point forward.

Figure 3 shows the acceleration response of mass 6 of the slip system to the impulsive force described previously. Also identified are the zero crossings, which were used as the zero times  $t_k$  in eq. (6). One can observe that the system dissipates quite a bit of energy in the first few cycles (before 20 ms) following which the response decays more gradually.

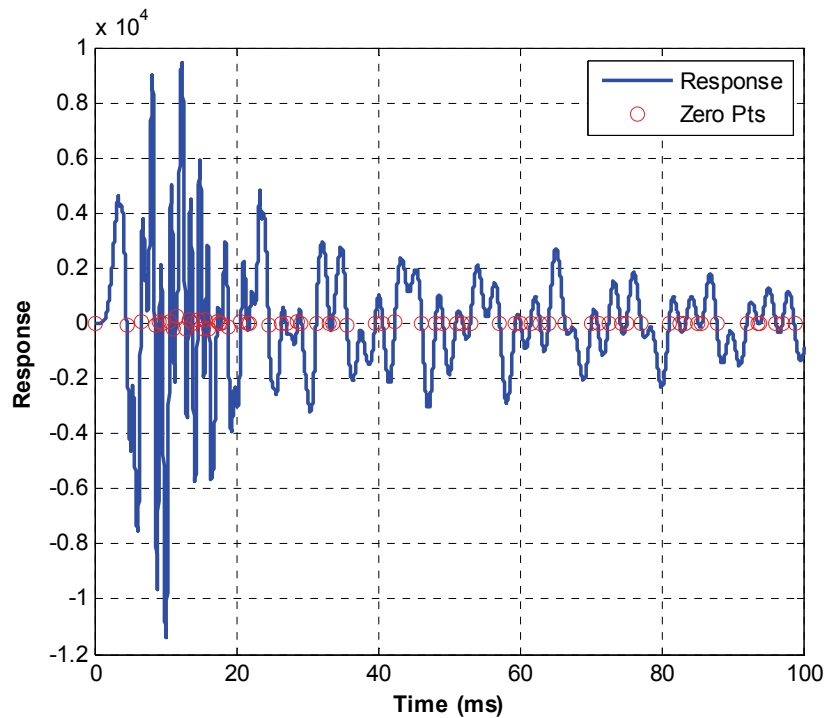


Figure 3: Initial portion of acceleration time response of system with slip nonlinearity. Red circles show the time instants used to create the ZEFFTs.

Figure 4 shows ZEFFTs of the response; one line is shown for each of the times shown with circles in Figure 3. The legend indicates  $t_k$  for each response, although some of the legend entries have been omitted for clarity. The responses exhibit significant changes in character in the 150 to 300 Hz frequency range for early times (zero times under about 30 milliseconds.) Most notably, the spectrum around the 180 and 230 Hz modes is lopsided for early zero times and then looks more as expected for a linear system after about 30ms.

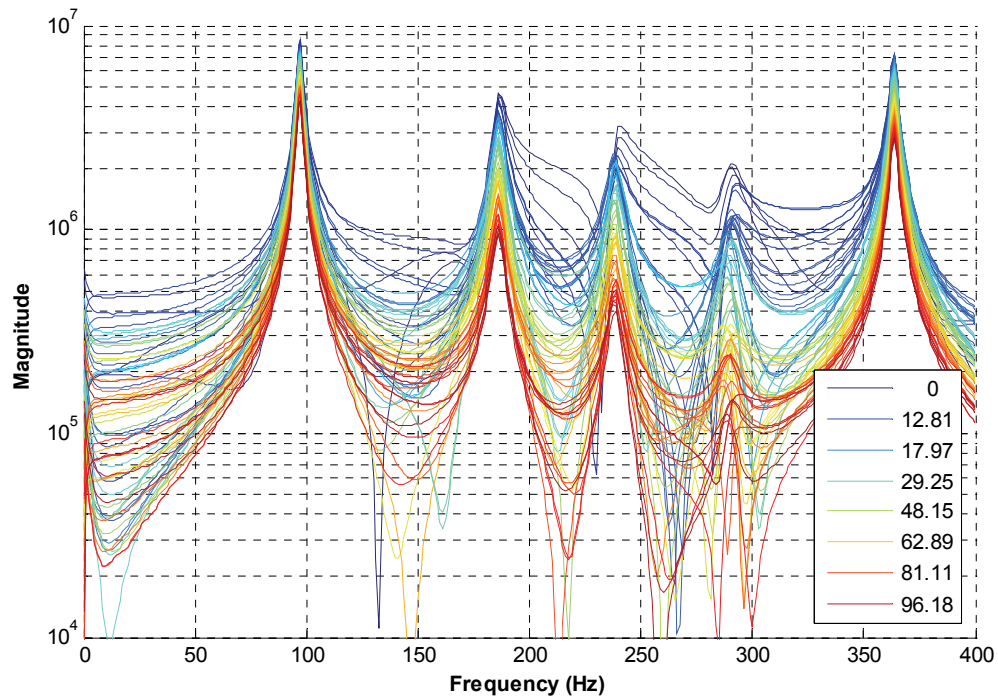


Figure 4: ZEFFTs of Acceleration for slip system for the time response in Figure 3.

Some of the responses in Figure 4 were curve fit and extrapolated backwards in time in order to compare them with the measured (nonlinear) responses from early times. An example of this is shown in Figure 5 where the response at 21.9 ms was curve fit and was then extrapolated back to 4.52 ms using eq. (8). (This was the earliest  $t_k$  in the set after the input had ceased.) The curve fit at 21.9ms, shown by a dotted red line, agrees very well to the response data at the same time, shown by a solid red line. However, there are marked differences between the extrapolation of this response and the data at 4.52 ms. First, the response data has much higher amplitude between the resonant peaks than does the linear system extrapolation. Also, the amplitude of the peak near 280 Hz is considerably lower in the extrapolation than in the measurement.

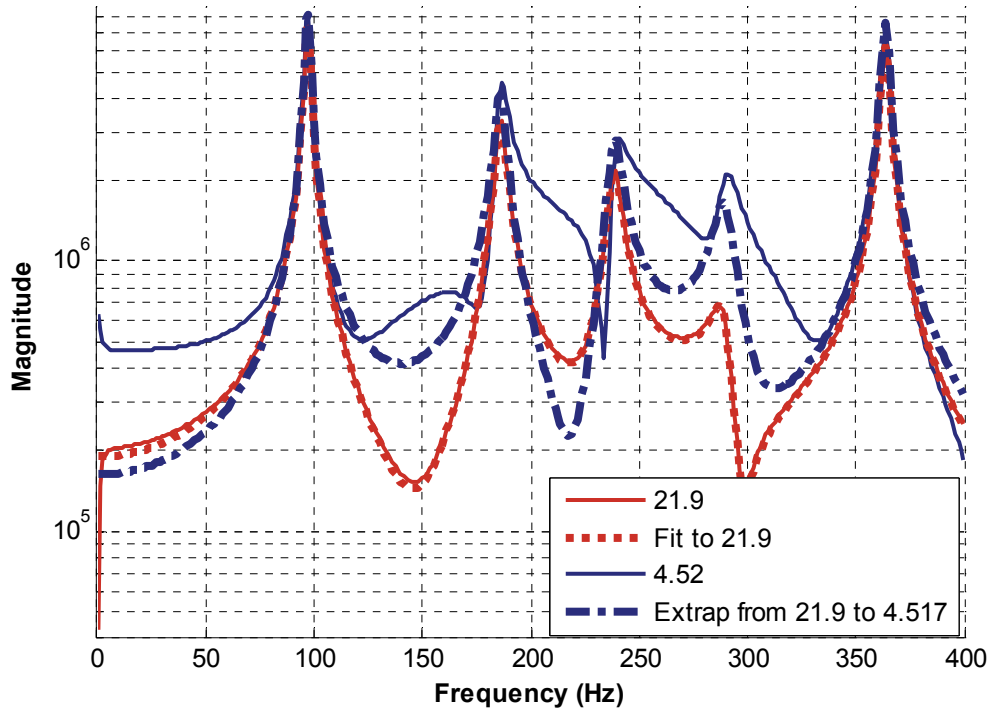


Figure 5: BEND - ZEFFTs of Accelerations for slip system zeroed up to 4.52ms and 21.9ms, curve fit at 21.9ms and extrapolation of the fit to 4.52ms.

The same procedure was repeated with the curve fit applied to the response at 97.1ms and then extrapolated to 29.2ms (not shown). In this case there was no discernible difference between the ‘measured’ response and the extrapolated response, suggesting that the system behaved linearly over this time period. The IBEND metric, given in Figure 6, characterizes this over all time using the curve fit for the 21.9ms ZEFFT, which was shown in Figure 5. The integral metric is small for all times later than 21.9ms, suggesting that the curve fit was accurate. Moving backwards in time, one observes that the curves begin to disagree at about 10 or 15 ms, suggesting that the system begins to behave nonlinearly at that time. (Marching forward in time, this is the instant at which nonlinear behavior ceased.)

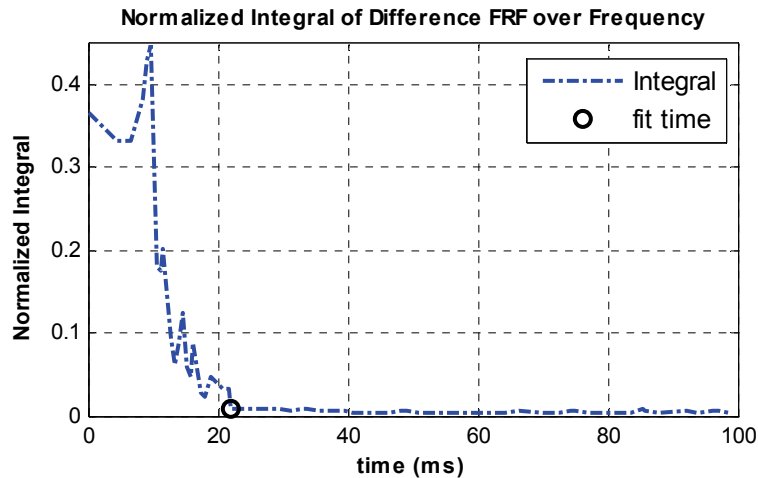


Figure 6: IBEND – metric for system with slip nonlinearity.

### 3.1.1. Discussion

One interesting feature of Figure 5 is the difference in the heights of the peaks in the measured and extrapolated responses at 280 Hz. The fact that the extrapolated response has lower amplitude than the measured response suggests that this mode dissipated energy due to the nonlinearity before the curve fit was performed (or else transferred it to another part of the spectrum). However, one must use care in interpreting this type of result, because the amplitudes of the peaks in the backwards extrapolation are very sensitive to the damping ratio identified (from the latter part of the time response), and damping can be difficult to estimate accurately. On the other hand, the extrapolation is helpful even if the damping estimate is questionable because it helps one to determine which features in the spectrum could not be described by a linear system model.

The true nonlinear behavior of this system was found by using the model to recreate the force in the nonlinear joint versus its displacement, as shown in Figure 7. This shows that the joint slips in two initial cycles all within 12ms of the impulse. Following those slip events, the joint behaves almost linearly oscillating between -1 and -3 mm displacement. This analytical result validates the insights obtained by the IBEND algorithm. Note that in most experiments a residual displacement such as this would be extremely difficult to measure due to the noise and insensitivity inherent in most transducers at zero frequency.

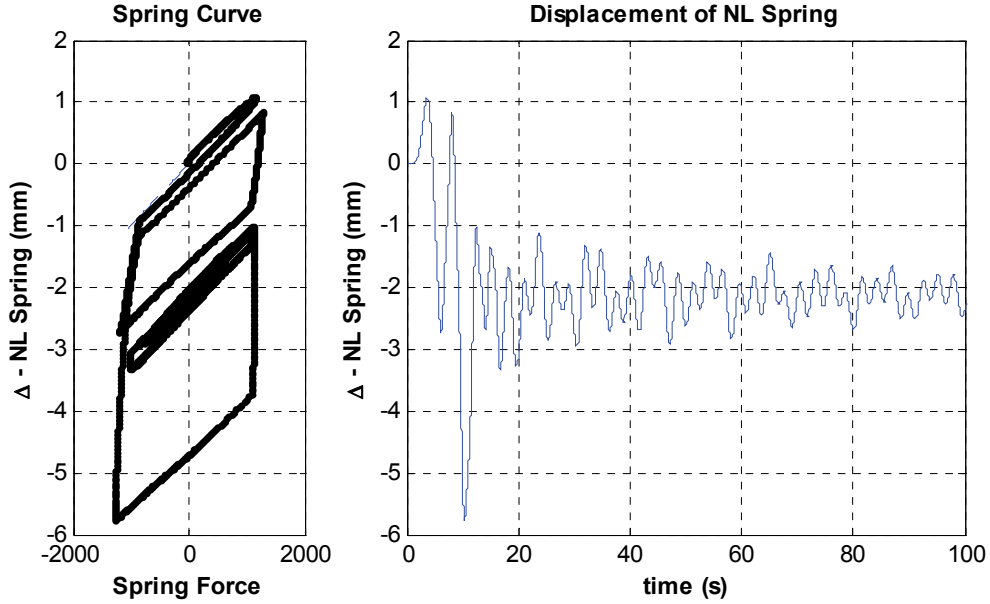


Figure 7: (left) Analytically generated plot of force versus displacement in the slip joint. (right) Displacement of nonlinear joint versus time.

The instants at which the ZEFFTs were created were shown in Figure 3. Those were all chosen to be instants when the response was near zero in order to reduce leakage effects in the ZEFFT plots of Figure 4. However, the authors have also obtained good results for the systems presented here using arbitrarily chosen starting points. The backwards extrapolation theory developed in Section 2 holds for any choice of starting points.

### 3.2. Contact Nonlinearity

The second case considers a model for contact nonlinearity in the joint connecting masses 2 and 6. The following force displacement law was used

$$f = \begin{cases} k_5 \Delta_5 + \beta k_5 \dot{\Delta}_5 & \Delta_5 < \Delta_{contact} \\ k_c k_5 \Delta_5 + \beta k_c k_5 \dot{\Delta}_5 & \Delta_5 \geq \Delta_{contact} \end{cases} \quad (10)$$

where  $\Delta_5 = (x_2 - x_6)$ ,  $k_5 = 1 \text{e}6 \text{ N/m}$  and  $k_c = 20$  is a unitless multiplicative factor that specifies how much the stiffness of the joint increases when contact occurs. The excitation energy  $E_{in}$  was 4e9 Joules.

Figure 8 shows the acceleration of mass 6 for this system, simulated using adaptive 4<sup>th</sup>-5<sup>th</sup> order Runge-Kutta integration to produce a response with a time step of 1.221e-4 seconds. To simulate a more realistic scenario, white noise was added to the response with a standard deviation equal to 2% of the



root-mean-square amplitude of the response. Large positive accelerations are seen in the early part of the time history due to the contact nonlinearity, while at later times the response is dominated by low frequency, lower amplitude oscillations.

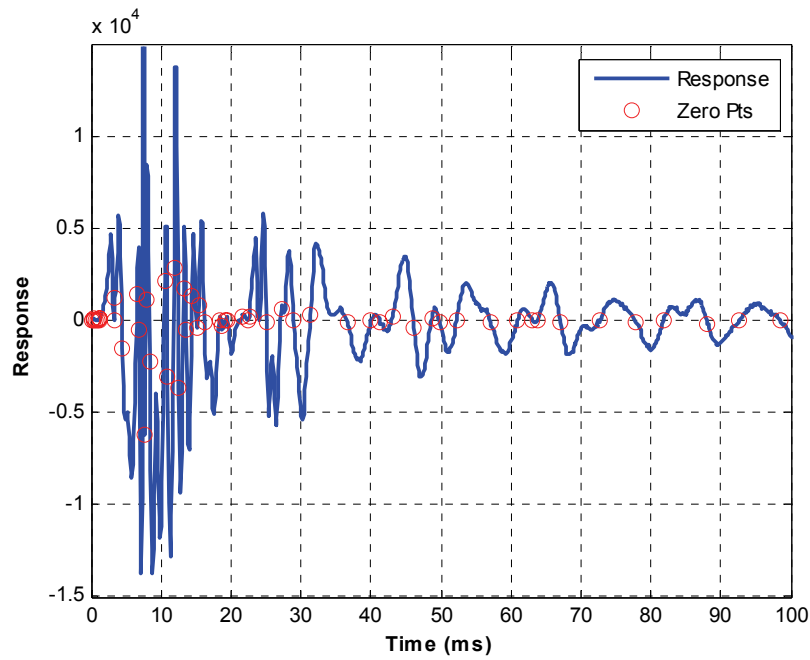


*Figure 8: Acceleration time response of system with contact nonlinearity and the time instants used to create the ZEFFTs.*

The ZEFFTs of the response in Figure 8 were computed and are shown in Figure 9. At early times there is clearly much more spectral energy both at the natural frequencies and throughout the entire frequency band. This energy appears to vanish after about 20ms so that four or five modes are visible in the response. The apparent noise in the response grows significantly with increasing time since the response amplitude is diminishing, especially at higher frequencies.

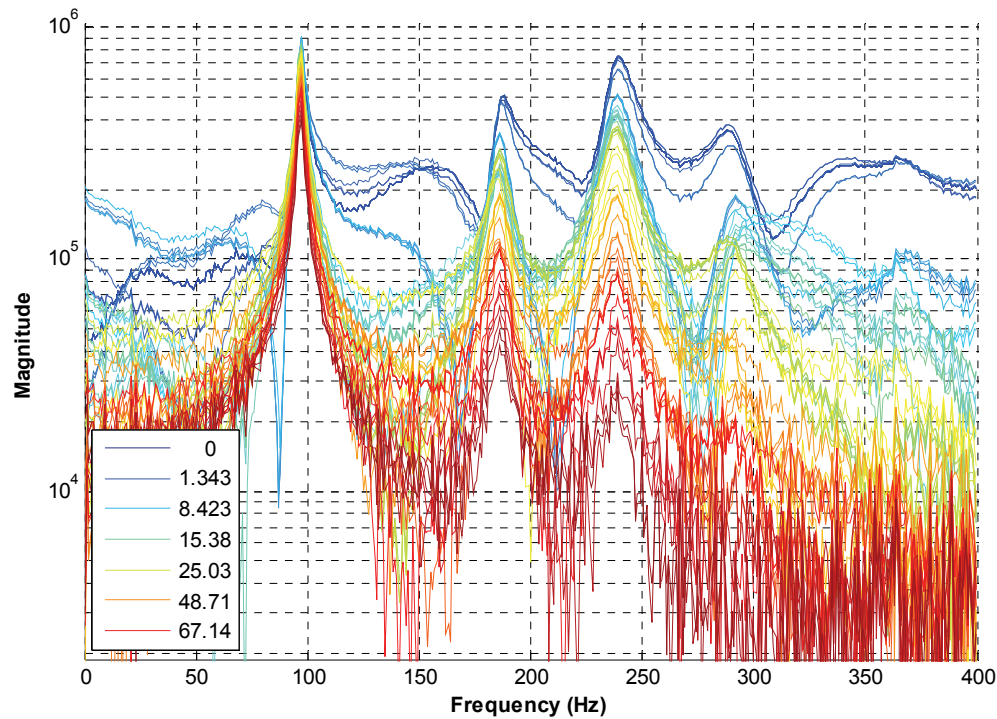


Figure 9: ZEFFTs of Acceleration for contact system, truncated at each of the time instants shown in Figure 8.

The responses in Figure 9 were curve fit in order to detect the end of nonlinear behavior. It was observed that the 290 and 370 Hz modes were difficult to identify in this response data. System identification was attempted at a few different zero times before good results were obtained. Figure 10 shows the curve fit to the response at 27.2ms and its extrapolation backwards to 1.34 ms and forwards to 81.8 ms. When the identification was performed on earlier ZEFFTs, spurious frequency content above 300 Hz masked the presence of the 370 Hz mode and contaminated the damping estimate for the 290 Hz mode. On the other hand, when ZEFFTs from times later than 80 ms were used in the identification, those modes had disappeared and could not be identified.

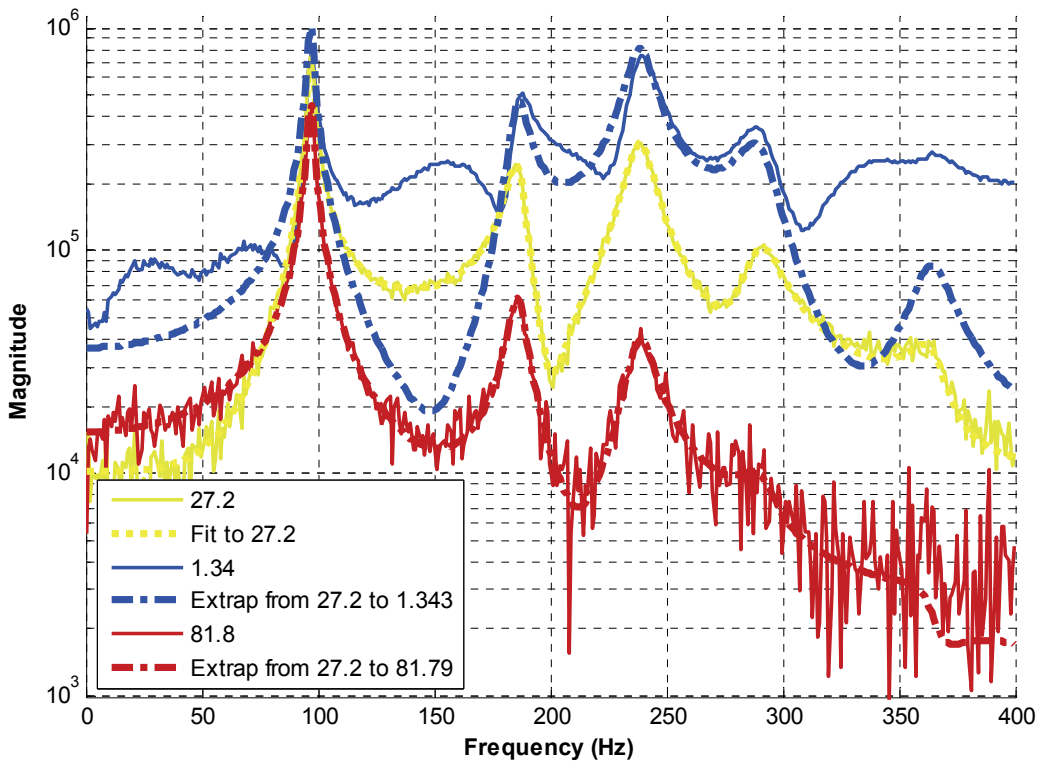


Figure 10: BEND - ZEFFTs of Accelerations for contact system truncated at 1.34, 27.2 and 81.8 ms, curve fit at 27.2 ms and extrapolation of the fit to 1.34 and 81.8 ms.

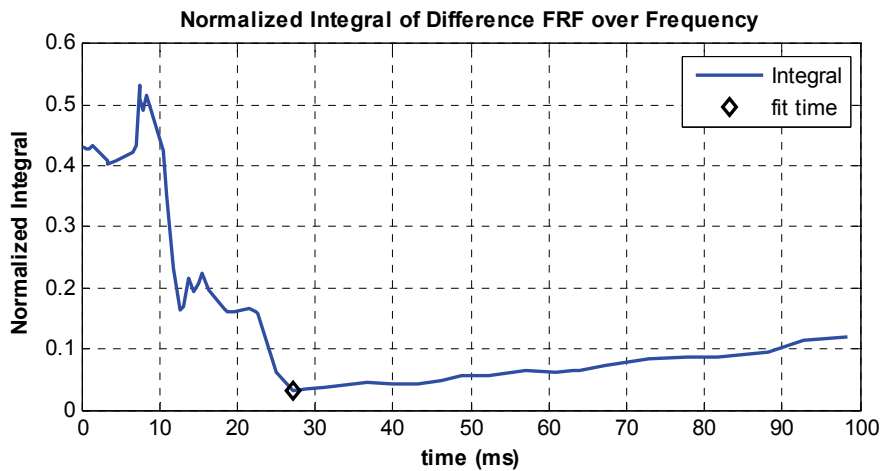


Figure 11: IBEND metric for contact system response data.

The IBEND metric for this contact system, computed using the ZEFFTs from 0 to 400 Hz, is shown in Figure 11. The integral is minimum around 25 ms and increases sharply moving towards earlier times, suggesting that there is significant nonlinear behavior that ends after 25 ms. The integral also

increases slightly going forward in time after 25 ms, indicating that the fit quality deteriorates at later times also.

### 3.2.1. Discussion

Once again, we can confirm these results using the analytical model. Figure 12 shows the displacement in the nonlinear joint both versus time and versus the force in the joint. This indicates that the last contact event occurs just before 25ms, although the negative amplitude responses suggest that the contacts that occur after 12 ms are much smaller than those that occur previously. The integral metric in Figure 11 shows a significant discrepancy before 25 ms, which becomes larger before 10 ms, agreeing with these observations. However, it was also noted that the integral metric increases slightly as time advances from the instant in which the curve fit was performed (25 ms). This phenomenon is to be expected when the response measurement is noisy. The signal-to-noise ratio of the measurement decreases as more of the initial, high-amplitude response is nullified, so one would expect the correlation between the fit and the measurement to deteriorate as well.

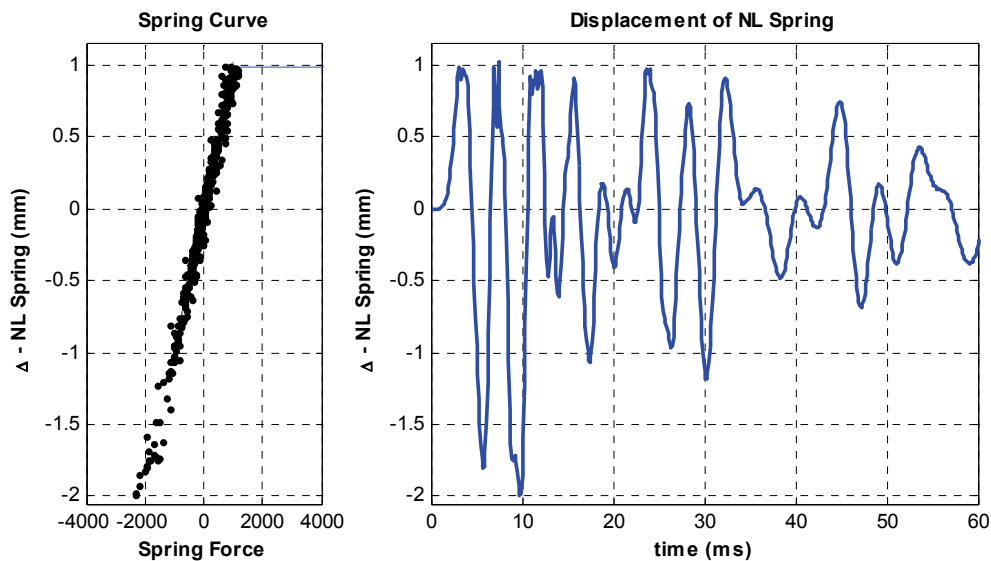


Figure 12: (left) Analytically generated plot of force versus displacement in nonlinear joint for contact system. (right) Displacement of nonlinear joint versus time.

It was noted that there was some difficulty in determining which of the frequency responses in Figure 9 should be used to identify the low-amplitude linear system in this case. In general, one can expect that it may often be necessary to attempt the curve fit at multiple zero times before identifying an

appropriate model. During this process, one would like to use late time responses in order to be sure that the nonlinearity is not active, but if data from very late times is used, then quickly decaying modes, may have already fallen below the noise threshold and hence may be difficult or impossible to identify. Such was the case with the 370 Hz mode in this data set. That mode vanished a short instant after which the nonlinearity disappeared, so it is difficult to be sure that the damping estimate for that mode was accurate. A different system might have a mode that vanishes completely before the nonlinearity disappears, so one must be cautious to assure that heavily damped linear modes are not erroneously mistaken for nonlinear behavior, especially when noise in the measurements is significant. Fortunately, the ZEFFTs may still help to interrogate the response, even if some regions of the spectra must be omitted from consideration due to these difficulties.

#### **4. Experimental Measurements**

This section explores the performance of the nonlinearity detection algorithm on experimental measurements. The system consists of a small electronic component that is bolted to larger conical structure. The system is freely suspended and subjected to a very short duration impulsive load. A modal test previously performed on the system identified several modes below 1kHz, all of which were lightly damped for low level modal test inputs. A measured time response of the system near the electronic component is shown in Figure 13, recorded with a sample frequency of 200 kHz.

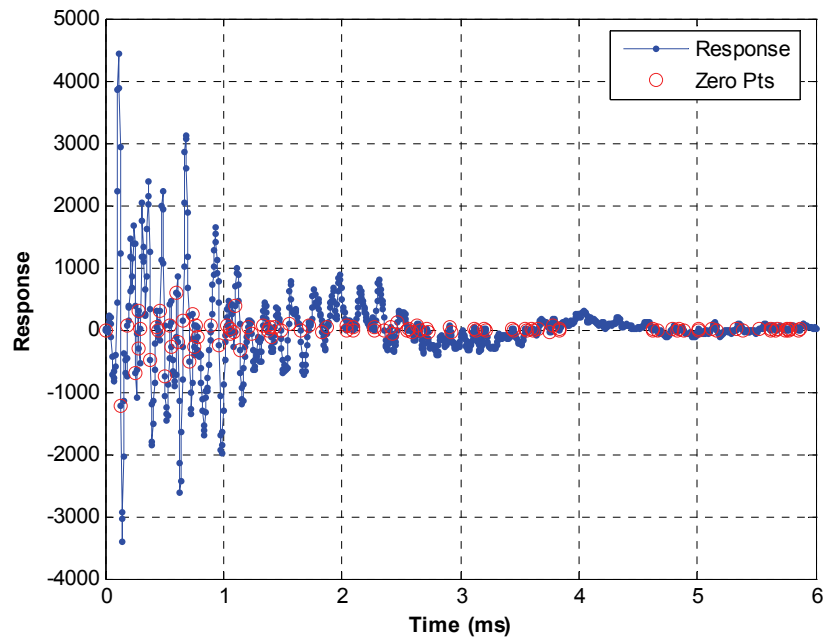


*Figure 13: Experimentally measured response on a subcomponent due to an impulsive load.*

The nonlinearity detection algorithm was applied at each of the zero crossings indicated with circles in Figure 13, and is shown in Figure 14. A broad peak is observed in the early time responses situated between 300 and 600 Hz, which does not appear to be typical of a linear system. This peak disappears after about 3.5ms, revealing a number of sharper peaks between 200 and 600 Hz.

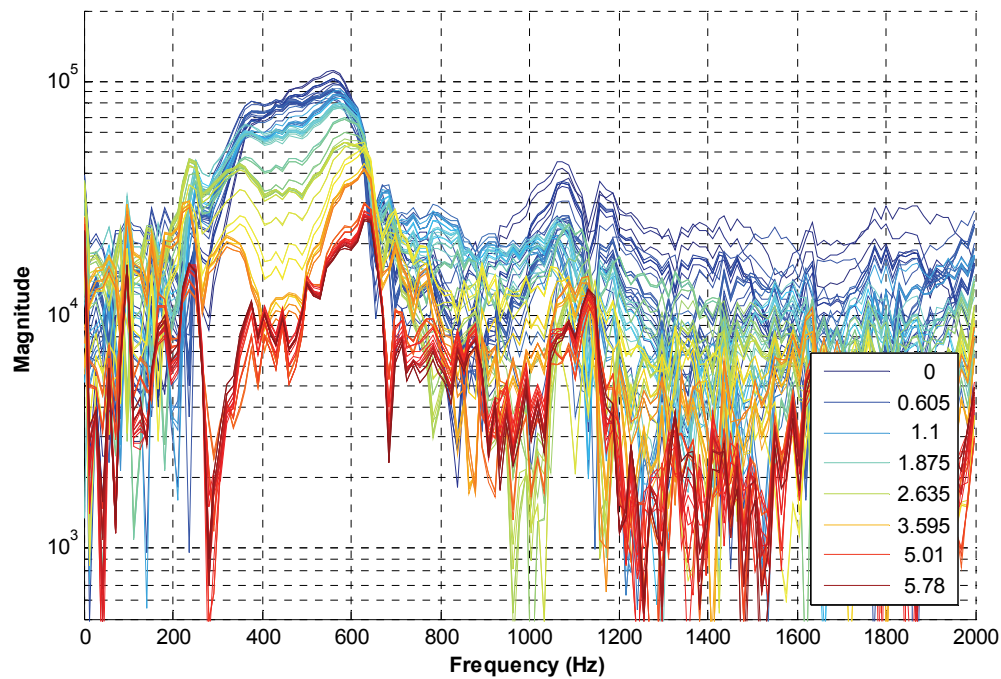


Figure 14: ZEFFTs of experimentally measured acceleration truncated at each of the zero crossings identified in Figure 13.

The AMI system identification algorithm was applied to the ZEFFT of the response at 3.84ms, identifying four modes below 800Hz. The curve fit and extrapolations to 0 and 5.87ms are shown in Figure 15, along with the corresponding measurements. Good agreement is seen both in the curve fit at 3.84ms and its extrapolation to 5.87ms below about 675 Hz, suggesting that the curve fit is reasonable and that the system behaves linearly over this time period. On the other hand, poor agreement is seen at 0ms, and one can see that an unreasonable number of linear modes would have to be added to the fit response before the curve fit could be made to agree with the measurement at 0ms. For example, the peak at 230 Hz is far too low in the measurement, so if the damping estimate for that mode is not greatly in error, then there must be another mode with a similar natural frequency that cancels that modes' response at 0ms, but which is not active later. The physics of the problem might rule out that possibility. Alternatively, if one accepts the hypothesis that the system is nonlinear, then the discrepancy in the heights of the peaks at 230 Hz can be explained by nonlinear dissipation or energy transfer to higher frequency modes.

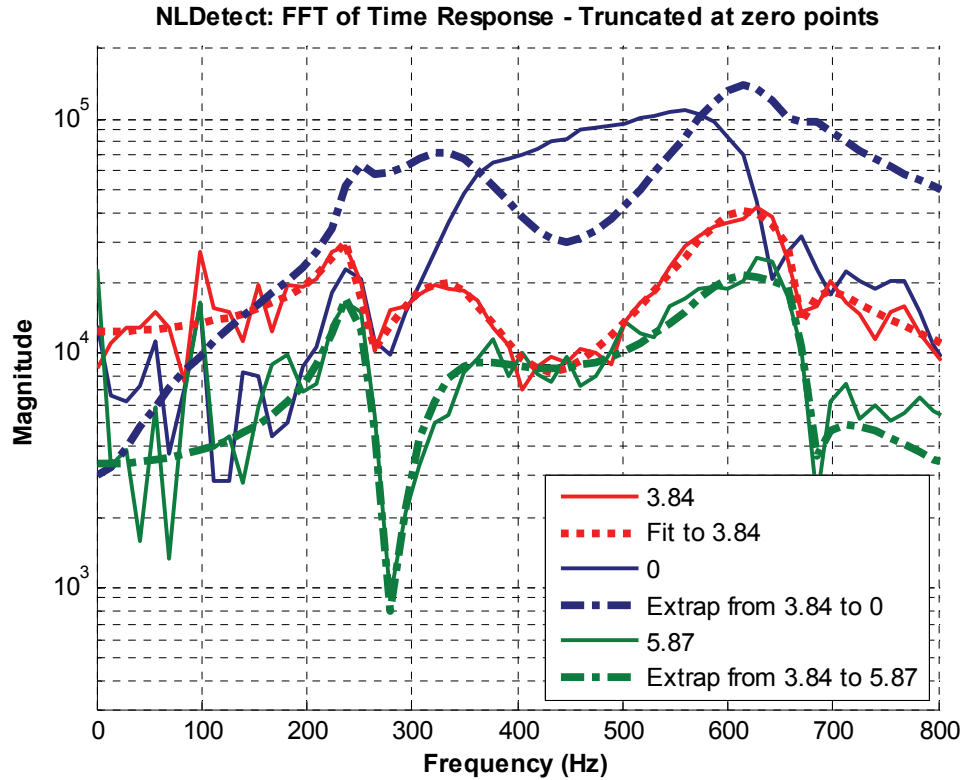


Figure 15: ZEFFTs of experimentally measured accelerations at 0, 3.84 and 5.87ms, curve fit at 3.84ms and extrapolation of the fit to 0 and 5.87ms.

The IBEND algorithm was applied to the data in the 200 to 650 Hz frequency band, and is shown in Figure 16. The integral metric suggests that the system behaves linearly after 2 ms. However, the IBEND metric also increases slightly as one marches forward in time from the curve fit instant (3.84 ms). This could indicate that the curve fit was somewhat inaccurate, or it may simply be a consequence of noise in the measurement, as was discussed in Section 3.2.1. The IBEND metric and the features in the ZEFFTs in Figure 15 both provide a strong indication that this system is behaving nonlinearly. The frequencies of the two dominant modes (at 330 and 620 Hz) seem to change with time in the ZEFFTs and the spectrum between these modes shows frequency content that does not seem to be describable by a reasonable number of linear modes. The peak in question is the dominant peak in the spectrum of the response, so one should model this system as nonlinear or else apply large safety factors to the linear models.



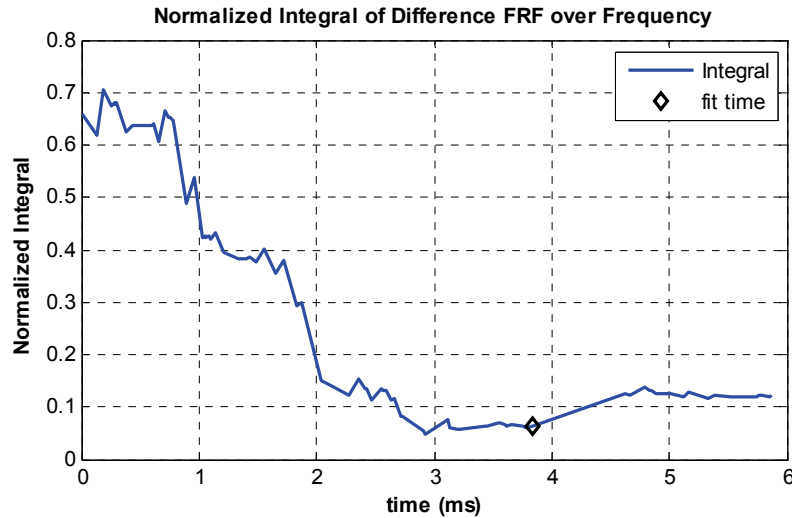


Figure 16: IBEND algorithm for experimental data using 200-650Hz frequency band.

## 5. Conclusions

This work has presented a set of tools that aid in detecting and characterizing nonlinearity in free response measurements and has evaluated them on both analytical and experimental acceleration data. The first tool, dubbed the Zeroed Early-time Fast Fourier Transform (ZEFFT), allows one to interrogate a free response and obtain a visual indication of the degree of nonlinear dynamic behavior in the response. This is done by inspecting the spectra of the response when varying portions of the initial response have been set to zero. When the system response is linear during some latter part of its free response, one can identify the low amplitude linear system and compare its response with the measured nonlinear response. This was dubbed the Backwards Extrapolation for Nonlinearity Detection or BEND algorithm, and was shown to be useful in clarifying the interpretation of the ZEFFTs. The BEND algorithm can also provide other information. For example, when applied to the analytical slip system the BEND algorithm identified a mode that seemed to dissipate a significant amount of energy due to the nonlinear forces. The last tool presented here was the integral of BEND (IBEND), which was shown to provide a single number measure of the degree of nonlinearity in the response.

Both analytical and experimental data have been considered to evaluate these tools. The analytical data illustrated that the algorithm can be used to accurately detect the time (or amplitude level) at which a system begins behaving linearly. This information may be useful when validating analytical models for slip or contact nonlinearity. The method also allows one to evaluate the degree of nonlinearity

in the response. Figure 5 showed that the response of the analytical slip system was not very different from its linear approximation while the other systems considered showed dramatic nonlinear behavior. The algorithm was also applied to experimental data from a system with a bolted joint. The measurement was very noisy, but some useful results were still obtained, demonstrating that the approach is robust to noise and the other limitations inherent to real experiments. The examples presented here have also shown that the algorithm may reveal which modes are most strongly affected by nonlinearity, reducing the effort required to perform subsequent nonlinear identification and analysis on the system.

These tools are valuable because they can be applied to relatively high order systems, even if the information obtained is more qualitative than quantitative. The experimental data used in Section 4 came from a system that has several modes in the frequency band of interest. However, only a few modes were significant in the response, so system identification was successful in the 200-650 Hz frequency band. The tools presented here proved very valuable in the test and analysis campaigns of that system, because they provided clear evidence that the system, which was initially thought to be linear, was actually behaving nonlinearly.

## 6. Acknowledgements

This work was performed, in part, at Sandia National Laboratories; Sandia is a multiprogram laboratory operated by Sandia Corporation, a Lockheed Martin Company, for the United States Department of Energy's National Nuclear Security Administration under Contract DE-AC04-94AL85000. The authors gratefully acknowledge Dan Segalman, Hartono Sumali, David Epp, Dan Gregory, Todd Simmermacher and Dane Quinn for their insight and suggestions regarding early drafts of this work.

## References

- [1] G. Kerschen, K. Worden, A. F. Vakakis, and J.-C. Golinval, "Past, present and future of nonlinear system identification in structural dynamics," *Mechanical Systems and Signal Processing*, vol. 20, pp. 505-592, 2006.
- [2] S. F. Masri and T. K. Caughey, "A Nonparametric Identification Technique for Nonlinear Dynamic Problems," *Journal of Applied Mechanics*, vol. 46, pp. 433-447, 1979.
- [3] K. Worden, J. R. Wright, M. A. Al-Hadid, and K. S. Mohammad, "Experimental Identification of Multi Degree-of-freedom Nonlinear Systems using Restoring Force Methods," *The International Journal of Analytical and Experimental Modal Analysis*, vol. 9, pp. 35-55, 1994.
- [4] D. E. Adams and R. J. Allemang, "Survey of Nonlinear Detection and Identification Techniques for Experimental Vibrations," in *International Seminar on Modal Analysis (ISMA 23)* Leuven, Belgium, 1998, pp. 269-281.

- [5] P. F. Pai and A. N. Palazotto, "HHT-Based Nonlinear Signal Processing Method for Parametric and Non-Parametric Identification of Dynamical Systems," *Int. J. Mechanical Sciences*, vol. 50, pp. 1619-1635, 2008.
- [6] D. Spina, C. Valente, and G. R. Tomlinson, "A New Procedure for Detecting Nonlinearity from Transient Data Using the Gabor Transform," *Nonlinear Dynamics*, vol. 11, pp. 235-254, 1996.
- [7] M. S. Allen and T. G. Carne, "Comparison of Inverse Structural Filter (ISF) and Sum of Weighted Accelerations Technique (SWAT) Time Domain Force Identification Methods," in *47th AIAA-ASME-ASCE-AHS-ASC Structures, Structural Dynamics, and Materials Conference* Newport, RI, 2006.
- [8] Q. Zhang, R. J. Allemang, and D. L. Brown, "Modal Filter: Concept and Applications," in *8th International Modal Analysis Conference (IMAC VIII)* Kissimmee, Florida, 1990, pp. 487-496.
- [9] G. Kerschen, A. F. Vakakis, Y. S. Lee, D. M. McFarland, and L. A. Bergman, "Toward a Fundamental Understanding of the Hilbert-Huang Transform in Nonlinear Structural Dynamics," in *24th International Modal Analysis Conference (IMAC XXIV)* St. Louis, Missouri, 2006.
- [10] J. H. Ginsberg, *Mechanical and Structural Vibrations*, First ed. New York: John Wiley and Sons, 2001.
- [11] M. S. Allen and J. H. Ginsberg, "A Global, Single-Input-Multi-Output (SIMO) Implementation of The Algorithm of Mode Isolation and Applications to Analytical and Experimental Data," *Mechanical Systems and Signal Processing*, vol. 20, pp. 1090-1111, 2006.
- [12] M. S. Allen and R. L. Mayes, "Comparison of FRF and Modal Methods for Combining Experimental and Analytical Substructures," in *25th International Modal Analysis Conference (IMAC XXV)* Orlando, Florida, 2007.
- [13] M. S. Allen, R. L. Mayes, and E. J. Bergman, "Experimental Modal Substructuring to Couple and Uncouple Substructures with Flexible Fixtures and Multi-point Connections," *Journal of Sound and Vibration*, vol. Submitted Aug 2009, 2010.
- [14] R. J. Allemang and D. L. Brown, "A Unified Matrix Polynomial Approach to Modal Identification," *Journal of Sound and Vibration*, vol. 211, pp. 301-322, 1998.
- [15] S. Maia, J. M. M. Silva, J. He, N. A. Lieven, R. M. Lin, G. W. Skingle, W. M. To, and A. P. V. Urgueira, *Theoretical and Experimental Modal Analysis*. Taunto, Somerset, England: Research Studies Press Ltd., 1997.
- [16] D. J. Ewins, *Modal Testing: Theory, Practice and Application*. Baldock, England: Research Studies Press, 2000.
- [17] B. Cauberghe, P. Guillaume, P. Verboven, S. Vanlanduit, and E. Parloo, "On the influence of the parameter constraint on the stability of the poles and the discrimination capabilities of the stabilisation diagrams," *Mechanical Systems and Signal Processing*, vol. 19, pp. 989-1014, September, 2005 2005.
- [18] M. V. Drexel and J. H. Ginsberg, "Mode Isolation: A New Algorithm for Modal Parameter Identification," *Journal of the Acoustical Society of America (JASA)*, vol. 110, pp. 1371-1378, Sept. 2001.
- [19] M. S. Allen and J. H. Ginsberg, "A linear least-squares version of the algorithm of mode isolation for identifying modal properties. Part II: Application and Assessment," *Journal of the Acoustical Society of America (JASA)*, vol. 116, pp. 908-915, 2004.
- [20] M. S. Allen and J. H. Ginsberg, "Global, Hybrid, MIMO Implementation of the Algorithm of Mode Isolation," in *23rd International Modal Analysis Conference (IMAC XXIII)* Orlando, Florida, 2005.
- [21] M. S. Allen and J. H. Ginsberg, "Modal Identification of the Z24 Bridge Using MIMO-AMI," in *23rd International Modal Analysis Conference (IMAC XXIII)* Orlando, Florida, 2005.
- [22] M. S. Allen and J. H. Ginsberg, "A Global, Single-Input-Multi-Output (SIMO) Implementation of The Algorithm of Mode Isolation and Applications to Analytical and Experimental Data," *Mechanical Systems and Signal Processing*, vol. 20, pp. 1090-1111, 2005.
- [23] J. H. Ginsberg and M. S. Allen, "A linear least-squares version of the algorithm of mode isolation for identifying modal properties. Part I: Conceptual development," *Journal of the Acoustical Society of America (JASA)*, vol. 116, pp. 900-907, 2004.
- [24] D. J. Segalman, "A Four-Parameter Iwan Model for Lap-Type Joints," *Journal of Applied Mechanics*, vol. 72, pp. 752-760, September 2005.